J. Fluid Mech. (1980), *vol.* 96, *part* 2, *pp.* 299–313
Printed in Great Britain

Local similarity solutions and their limitations

By H. K. MOFFATT AND B. R. DUFFY
School of Mathematics, University of Bristol, England

(Received 15 March 1979)

Two problems exhibiting breakdown in local similarity solutions are discussed, and the appropriate asymptotic form of the exact solution is determined in each case. The first problem is the very elementary problem of pressure driven flow along a duct whose cross-section has a sharp corner of angle 2α. When $2\alpha < \frac{1}{2}\pi$, a local similarity solution is valid, whereas, when $2\alpha > \frac{1}{2}\pi$, the solution near the corner depends on the global geometry of the cross-section. The transitional behaviour when $2\alpha = \frac{1}{2}\pi$ is determined.

The second problem concerns low-Reynolds-number flow in the wedge-shaped region $|\theta| < \alpha$ when either a normal velocity proportional to distance from the vertex is imposed on both boundaries, or a finite flux $2Q$ is introduced or extracted at the vertex (the Jeffery–Hamel problem). It is shown that the similarity solution in either case is valid only when $2\alpha < 2\alpha_c \approx 257{\cdot}5°$; a modified problem is solved exactly revealing the behaviour when $\alpha > \alpha_c$, and the transitional behaviour when $\alpha = \alpha_c$ (when the similarity solutions become infinite everywhere). An interesting conclusion for the Jeffery–Hamel problem is that when $\alpha > \alpha_c$, inertia forces are of dominant importance throughout the flow field no matter how small the source Reynolds number $2Q/\nu$ may be.

1. Introduction

Consider Poiseuille flow along a straight duct of cross-section $\mathscr{D}$. Choosing co-ordinates $Oxyz$ with Oz parallel to the flow, the equation for the velocity $w(x, y)$ is

$$\nabla^2 w = -G/\mu \quad \text{in} \quad \mathscr{D}, \tag{1.1}$$

where G is the applied pressure gradient, and μ the viscosity of the fluid. The boundary condition is

$$w = 0 \quad \text{on} \quad \partial\mathscr{D}. \tag{1.2}$$

If the boundary $\partial\mathscr{D}$ has any sharp corners (as is the case if, for example, it has square or triangular cross-section), then it is very natural to enquire into the nature of the solution of the problem (1.1), (1.2) near the corner. Choosing polar co-ordinates (r, θ) with origin at the corner and with $\theta = 0$ along the bisector of the angle, so that locally the boundary consists of the two planes $\theta = \pm\alpha$ (figure 1), one might reasonably conjecture that w must have a local similarity form depending only on r, θ, G/μ and α (i.e. independent of the 'remote' geometry of the duct). If this is so, then on dimensional grounds,

$$w \sim (G/\mu) r^2 f(\theta) \tag{1.3}$$

0022-1120/80/4360-8100 $02.00

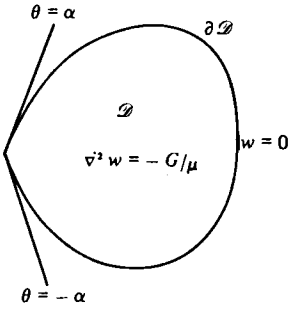

FIGURE 1. Poiseuille flow along duct whose cross-section $\mathscr{D}$ has a corner of angle 2α.

(the dependence on α being implicit), and the only possible form of $f(\theta)$ compatible with (1.1) and (1.2) is

$$f(\theta) = \frac{1}{4}\left(\frac{\cos 2\theta}{\cos 2\alpha} - 1\right). \tag{1.4}$$

This solution 'explodes' when $2\alpha = \frac{1}{2}\pi$ (and also when $2\alpha = \frac{3}{2}\pi$), and this leads one to question the validity of the above conjecture.† It is physically clear that the solution must remain finite when $2\alpha = \frac{1}{2}\pi$, and that the similarity form (1.3) cannot therefore be correct for this angle. The difficulty is in fact quite an elementary one, and we shall resolve it in § 2.

A similar difficulty, which may be described as an inapplicability of a local similarity solution, can however arise in more complex physical contexts, when the means of resolution of the problem may not be so readily apparent. A second example, which we shall treat in §§ 3–5, is the following. Suppose that viscous fluid is contained in the space $|\theta| < \alpha$ between two planes $\theta = \pm\alpha$ which are hinged at their intersection (so that the angle α may be varied), and suppose that the normal velocity is instantaneously prescribed on the planes, by rotating the planes about O as indicated in figure 2(*a*), as

$$u_\theta = \mp r\omega \quad \text{on} \quad \theta = \pm\alpha. \tag{1.5}$$

† A similar breakdown was noted by Fraenkel (1961) in the context of inviscid corner flow with constant vorticity; Fraenkel correctly resolved the behaviour when $2\alpha = \frac{1}{2}\pi$, but, by limiting attention to acute angles, the inapplicability of the similarity solution for $2\alpha > \frac{1}{2}\pi$ (see § 2 below) was not explicitly appreciated.

The problem has been touched on in a number of other studies, but the particular difficulty discussed here does not appear to have been explicitly recognized. For example, Collins & Dennis (1976) study flow along a curved duct of triangular cross-section, and they consider particularly the case of a right-angled triangle. They state that the solution of (1.1) is $O(r^2)$ near $r = 0$ 'regardless of the angle of the corner', but, as suggested by (1.4), and as demonstrated in § 2 below, this is not true when $2\alpha \geqslant \frac{1}{2}\pi$ (although the subsequent argument of Collins & Dennis remains substantially unaffected).

A second example is provided by the work of Allen & Biggin (1974) who studied the flow of a liquid filament down an inclined plane, the shape of the free surface being controlled by surface tension and the contact angle at the 3-phase contact line. When this contact angle is α, a local analysis using a zero stress condition on the free surface $\theta = 0$ and a no-slip condition on the solid boundary $\theta = \alpha$ again yields (1.4), which breaks down when $\alpha = \frac{1}{4}\pi$. Allen & Biggin in fact chose $\alpha = \frac{1}{4}\pi$ in their numerical computation of the velocity distribution over the cross-section of the filament; a finite element procedure provided an apparently well-behaved solution. It was in fact through attempting to understand the structure of this solution that we were led to investigate the paradox presented by (1.4) when $\alpha = \frac{1}{4}\pi$.

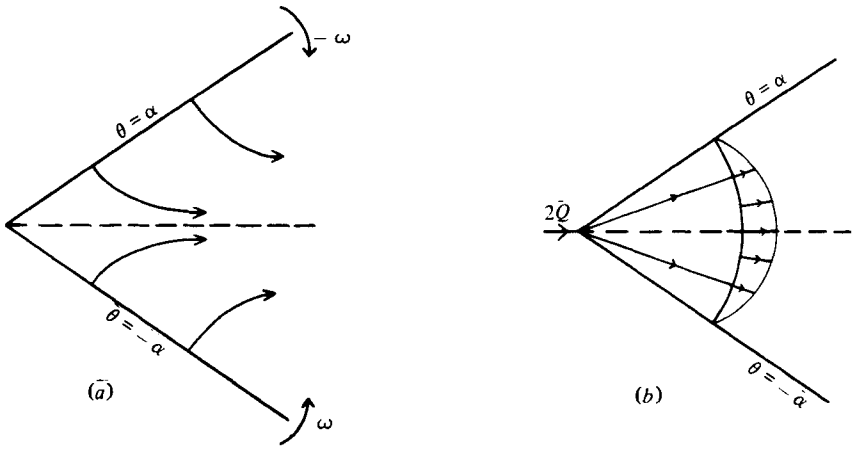

FIGURE 2. (*a*) The hinged plate problem, $\omega r^2/\nu \ll 1$.
(*b*) The Jeffery–Hamel problem, $Q/\nu \ll 1$.

Sufficiently near O, inertia is clearly negligible, and the stream function $\psi(r,\theta)$ satisfies the biharmonic equation

$$\nabla^4\psi = 0 \tag{1.6}$$

and the boundary conditions

$$\frac{\partial\psi}{\partial\theta} = 0, \quad \frac{\partial\psi}{\partial r} = \pm r\omega \quad \text{on} \quad \theta = \pm\alpha. \tag{1.7}$$

Again it is tempting to seek a similarity solution for ψ depending only on ω, r, θ and α; on dimensional grounds this must have the form

$$\psi = \tfrac{1}{2}\omega r^2 f(\theta), \tag{1.8}$$

and the unique function $f(\theta)$ compatible with (1.6) and (1.7) (Moffatt 1964*a*) is

$$f(\theta) = \frac{\sin 2\theta - 2\theta\cos 2\alpha}{\sin 2\alpha - 2\alpha\cos 2\alpha}. \tag{1.9}$$

This solution explodes when $\tan 2\alpha = 2\alpha$, i.e. when $2\alpha = 257{\cdot}45°$. For this critical angle, $f(\theta)$ apparently becomes infinite for *all* $|\theta| < \alpha$, and the corresponding velocity components derived from (1.8) become infinite also. The assertion that the Reynolds number is low near the corner therefore requires re-examination, as does the relevance of a similarity solution of the form (1.8).

A closely related difficulty has been noted (Fraenkel 1962) in the context of the low Reynolds number limit of the Jeffery–Hamel problem (Batchelor 1967, §5.6). Suppose that the planes $\theta = \pm\alpha$ are fixed and that fluid is introduced at a volume rate $2Q$ (per unit length) at the intersection (figure 2*b*); in this case, the low Reynolds number limit of the Jeffery–Hamel stream function (which provides an exact solution of the Navier–Stokes equations) is

$$\psi = Q\frac{\sin 2\theta - 2\theta\cos 2\alpha}{\sin 2\alpha - 2\alpha\cos 2\alpha}, \tag{1.10}$$

with precisely the same angular dependence as (1.8) and the same pathological behaviour at $2\alpha \approx 257°$

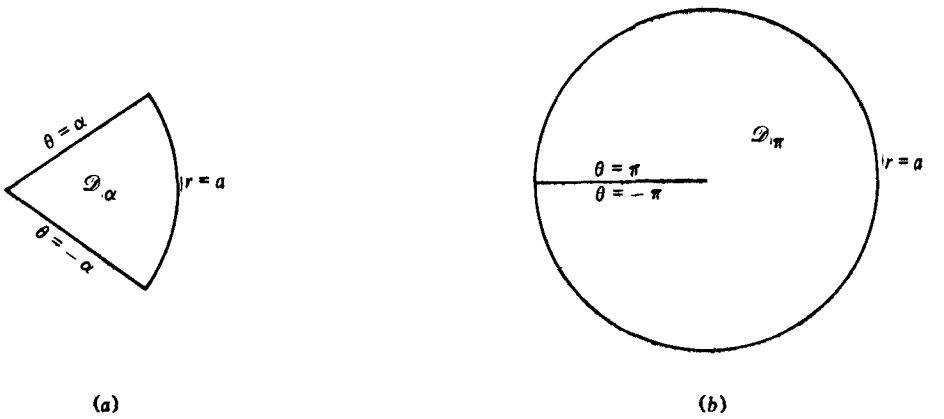

(*a*) (*b*)

FIGURE 3. The sector geometry considered in § 2.

The same type of difficulty has been encountered and resolved in an entirely different physical context by Sternberg & Koiter (1958). When an elastic wedge is subjected to a couple that is concentrated at the vertex, the displacement field (which may be derived from a function satisfying the biharmonic equation) involves the same factor $(\sin 2\alpha - 2\alpha\cos 2\alpha)^{-1}$ which blows up at $2\alpha \approx 257°$. Sternberg & Koiter resolved this apparently paradoxical behaviour by spreading out the force field providing the couple over a small neighbourhood of the vertex and solving the resulting problem exactly. We shall follow a similar procedure in the fluid context in §§ 3–5, and shall in this way provide a simultaneous resolution of the hinged plate and Jeffery–Hamel paradoxes.

2. The Poiseuille problem at a sharp corner

Consider the problem defined by (1.1) and (1.2) when $\mathscr{D}\,(=\mathscr{D}_\alpha)$ is the domain bounded by the lines $\theta = \pm\alpha$ and the circular arc $r = a$. We may consider the full range of angles $0 < 2\alpha \leqslant 2\pi$, the limiting case $2\alpha = 2\pi$ representing a circular pipe with a radial 'flange' (figure 3).

Suppose first that $2\alpha \neq \frac{1}{2}\pi$ or $\frac{3}{2}\pi$. Then the general solution of (1.1) symmetric about $\theta = 0$ and satisfying $w = 0$ on $\theta = \pm\alpha$ is

$$w = \frac{Gr^2}{4\mu}\left(\frac{\cos 2\theta}{\cos 2\alpha} - 1\right) + \sum_{n=0}^{\infty} A_n r^{\lambda_n}\cos\lambda_n\theta, \tag{2.1}$$

where

$$\lambda_n\alpha = \tfrac{1}{2}(2n+1)\pi, \quad n = 0, 1, 2, \ldots. \tag{2.2}$$

The coefficients A_n are determined by the condition $w = 0$ on $r = a$ ($|\theta| < \alpha$); using the orthogonality condition

$$\int_{-\alpha}^{\alpha} \cos\lambda_n\theta\cos\lambda_m\theta\,d\theta = \alpha\delta_{nm}, \tag{2.3}$$

we find

$$A_n = \frac{(-1)^{n+1}\,2Ga^{2-\lambda_n}}{\alpha\mu\lambda_n(\lambda_n^2 - 4)}. \tag{2.4}$$

Now $\lambda_0 = \pi/2\alpha$, so that $\lambda_0 \gtrless 2$ according as $2\alpha \lessgtr \frac{1}{2}\pi$. Hence the particular integral

$$w_0(r,\theta) = \frac{Gr^2}{4\mu}\left(\frac{\cos 2\theta}{\cos 2\alpha} - 1\right) \tag{2.5}$$

is the dominant part of the solution (2.1) near $r = 0$ *only if* $2\alpha < \frac{1}{2}\pi$. If $2\alpha > \frac{1}{2}\pi$, the solution is dominated near $r = 0$ by the leading term of the series of eigenfunctions, namely

$$w \sim A_0 r^{\lambda_0}\cos\lambda_0\theta = \frac{16Ga^2\alpha^2}{\mu\pi(16\alpha^2-\pi^2)}\left(\frac{r}{a}\right)^{\pi/2\alpha}\cos\frac{\pi\theta}{2\alpha}, \quad 2\alpha > \tfrac{1}{2}\pi. \tag{2.6}$$

The particular value of the coefficient A_0 depends on the 'global' geometry of $\mathscr{D}$, and so the asymptotic form (2.6) cannot be obtained from purely local considerations.

When $2\alpha > \frac{3}{2}\pi$, λ_0 and λ_1 are both less than 2, and so the first *two* terms of the series in (2.1) both dominate over $w_0(r,\theta)$ for small r. In the extreme case $2\alpha = 2\pi$ (figure 3*b*), we find

$$w \sim \frac{16Ga^2}{3\mu\pi}\left[\frac{1}{5}\left(\frac{r}{a}\right)^{\frac{1}{2}}\cos\tfrac{1}{2}\theta - \frac{1}{7}\left(\frac{r}{a}\right)^{\frac{3}{2}}\cos\tfrac{3}{2}\theta + O(r^2)\right]. \tag{2.7}$$

The cases $2\alpha = \frac{1}{2}\pi$ and $\frac{3}{2}\pi$ require special attention. If we let $2\alpha = \frac{1}{2}\pi + \epsilon$ in the expression (2.1), we find

$$w \sim -\frac{Gr^2}{4\mu}\left[1 + \frac{1}{\epsilon}\left(\cos 2\theta - \left(\frac{r}{a}\right)^{-4\epsilon/\pi}\cos\left(2 - \frac{4\epsilon}{\pi}\right)\theta\right)\right] + \sum_{n=1}^{\infty} A_n r^{\lambda_n}\cos\lambda_n\theta,$$

so that, in the limit $\epsilon \to 0$ (i.e. $2\alpha = \frac{1}{2}\pi$),

$$w = -\frac{Gr^2}{\pi\mu}\left[\frac{\pi}{4} + \left(\log\frac{r}{a}\right)\cos 2\theta - \theta\sin 2\theta\right] + \sum_{n=1}^{\infty} A_n r^{\lambda_n}\cos\lambda_n\theta. \tag{2.8}$$

2α	Leading terms in expansion of w near $r = 0$
$0 < 2\alpha < \frac{1}{2}\pi$	r^2, then $r^{\pi/2\alpha}$
$2\alpha = \frac{1}{2}\pi$	$r^2\log r$, then r^2, then r^6
$\frac{1}{2}\pi < 2\alpha < \frac{3}{2}\pi$	$r^{\pi/2\alpha}$, then r^2, then $r^{3\pi/2\alpha}$
$2\alpha = \frac{3}{2}\pi$	$r^{\frac{2}{3}}$, then $r^2\log r$, then r^2, then $r^{\frac{10}{3}}$
$\frac{3}{2}\pi < 2\alpha \leqslant 2\pi$	$r^{\pi/2\alpha}$, then $r^{3\pi/2\alpha}$, then r^2, then $r^{5\pi/2\alpha}$

TABLE 1

A similar treatment of the neighbourhood of $2\alpha = \frac{3}{2}\pi$ shows that, when $2\alpha = \frac{3}{2}\pi$,

$$w = -\frac{Gr^2}{3\pi\mu}\left[\frac{3\pi}{4} - \left(\log\frac{r}{a}\right)\cos 2\theta + \theta\sin 2\theta\right] + \frac{9Ga^2}{8\pi\mu}\left(\frac{r}{a}\right)^{\frac{2}{3}}\cos\tfrac{2}{3}\theta + \sum_{n=2}^{\infty} A_n r^{\lambda_n}\cos\lambda_n\theta. \tag{2.9}$$

In this case, the singularity in $w_0(r,\theta)$ is compensated by an equal and opposite singularity in the second term ($n = 1$) of the series in (2.1).

The above results concerning the leading terms in the asymptotic expansion of $w(r,\theta)$ near $r = 0$ are summarized in table 1.

As noted in the footnote on p. 300, the same type of mathematical problem has

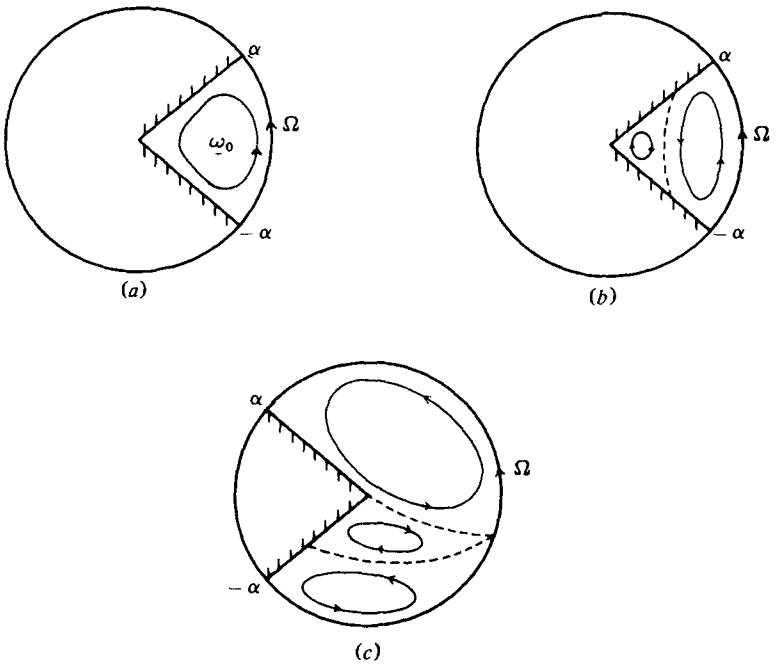

FIGURE 4. Flow generated in domain $\mathscr{D}_\alpha$ by rotation of bounding cylinder keeping $\theta = \pm\alpha$ fixed: (*a*) assuming no separation; (*b*) and (*c*), likely streamline patterns allowing for boundary-layer separation.

been considered by Fraenkel (1961) in a different physical context. An example of the sort of situation envisaged by Fraenkel (who limited attention to acute angles $2\alpha \leqslant \frac{1}{2}\pi$) is indicated in figure 4(*a*), which shows a method of generating a flow with closed streamlines in the domain $\mathscr{D}_\alpha$, by rotation of the cylinder $r = a$ with angular velocity Ω, keeping the radial boundaries $\theta = \pm\alpha$ fixed. If $R = \Omega a^2/\nu \gg 1$, *and if the flow does not separate* from the boundary at any point, then the vorticity ω is uniform throughout the core region (Batchelor 1956) – $\omega = \omega_0$ say – and the stream function $\psi(r, \theta)$ is determined by

$$\nabla^2\psi = -\omega_0 \quad \text{in} \quad \mathscr{D}_\alpha, \quad \psi = 0 \quad \text{on} \quad \partial\mathscr{D}_\alpha. \tag{2.10}$$

The solution for ψ is then precisely analogous to the solution for $w(r, \theta)$ described above. The above proviso concerning non-separation is however physically unrealistic. If $2\alpha < \pi$, the flow will separate at some point on $\theta = \alpha$ where the pressure gradient impressed on the boundary layer is adverse (figure 4*b*)†; and if $2\alpha > \pi$, the flow will separate at the sharp vertex (figure 4*c*). In either case, the vorticity will take different constant values in different subdomains of $\mathscr{D}_\alpha$ separated by thin layers in which viscous forces are non-negligible; the specification (2.10) is then clearly inapplicable.

† The secondary eddy so formed will then also presumably separate when R is sufficiently large; and indeed, when $R \to \infty$, the limiting steady solution presumably involves an infinite sequence of eddies, within each of which the vorticity takes a different constant value.

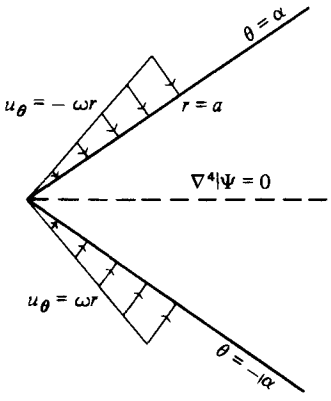

FIGURE 5. Modified Jeffery–Hamel problem treated in §§ 3–5. The hinged plate problem is obtained in the limit $a \to \infty$, and the conventional Jeffery–Hamel problem in the limit $a \to 0$, $\omega \to \infty$, $Q = \frac{1}{2}\omega a^2 = \text{constant}$.

3. A modified Jeffery–Hamel problem

Consider now the following modification of the Jeffery–Hamel problem (figure 5): suppose that viscous fluid is contained in the space $|\theta| < \alpha$ between the planes $\theta = \pm\alpha$ on which the radial velocity is zero and the normal velocity u_θ is specified as

$$u_\theta = \begin{cases} \mp \omega r & r < a, \\ 0 & r > a. \end{cases} \tag{3.1}$$

The total flux introduced into the region $|\theta| < \alpha$ is then

$$2Q = 2\int_0^a \omega r \, dr = \omega a^2. \tag{3.2}$$

The 'hinged plate' problem described in § 1 is obtained in the limit $a \to \infty$, and the Jeffery–Hamel problem is obtained by the limiting process $a \to 0$, $\omega \to \infty$, with Q constant.

The stream function $\psi(r, \theta)$ satisfies the biharmonic equation

$$\nabla^4 \psi = 0 \tag{3.3}$$

and the boundary conditions

$$\frac{\partial \psi}{\partial \theta} = 0, \quad \frac{\partial \psi}{\partial r} = \begin{cases} \pm \omega r & r < a \\ 0 & r > a \end{cases} \quad \text{on} \quad \theta = \pm\alpha. \tag{3.4}$$

This problem may be solved by means of the Mellin transform (cf. Tranter 1948, Sternberg & Koiter 1958, who considered problems involving elastic wedges, and Moffatt 1964*b* in which a similar problem with specified *tangential* velocity on $\theta = \pm\alpha$ was treated). This is defined by

$$\overline{\psi}(p, \theta) = \int_0^\infty r^{p-1} \psi(r, \theta) \, dr, \tag{3.5}$$

with inverse relation

$$\psi(r, \theta) = \frac{1}{2\pi i} \int_{c-i\infty}^{c+i\infty} r^{-p} \overline{\psi}(p, \theta) \, dp. \tag{3.6}$$

In (3.5), p may be complex, its real part being such that the integral exists; clearly, provided

$$\psi(r,\theta) = \begin{cases} o(r^{1+\epsilon}) & \text{as} \quad r \to 0, \\ o(r^{1-\epsilon}) & \text{as} \quad r \to \infty, \end{cases} \tag{3.7}$$

where $\epsilon > 0$, the integral (3.5) will certainly exist in a neighbourhood of the line $\mathrm{Re}\, p = -1$ in the complex p plane†. We shall find that $c = -1$ is an appropriate choice for the real constant c in (3.6). The various operations that follow may all be justified under the conditions (3.7), which may be verified retrospectively.

Under these conditions, equation (3.3) transforms to

$$\frac{d^4\overline{\psi}}{d\theta^4} + [(p+2)^2 + p^2]\frac{d^2\overline{\psi}}{d\theta^2} + p^2(p+2)^2\overline{\psi} = 0, \tag{3.8}$$

and the boundary conditions (3.4) transform to

$$\left.\begin{aligned} \frac{d\overline{\psi}}{d\theta} &= 0, \\ \overline{\psi} &= \mp\frac{\omega}{p(p+2)}a^{p+2}, \end{aligned}\right\} \quad \text{on} \quad \theta = \pm\alpha. \tag{3.9}$$

The (unique) solution of (3.8) and (3.9) is

$$\overline{\psi}(p,\theta) = \frac{\omega a^{p+2}}{W(p)}\left[\frac{\cos(p+2)\alpha \sin p\theta}{p} - \frac{\cos p\alpha \sin(p+2)\theta}{p+2}\right], \tag{3.10}$$

where

$$W(p) = (p+1)\sin 2\alpha - \sin 2(p+1)\alpha. \tag{3.11}$$

Note that

$$W(-p) = -W(p-2) \tag{3.12}$$

and that

$$\overline{\psi}(-p,\theta) = a^{-2(p-1)}\overline{\psi}(p-2,\theta). \tag{3.13}$$

It follows from (3.6) (with $c = -1$) that

$$\psi(r,\theta) = (r/a)^2\psi(a^2/r,\theta). \tag{3.14}$$

It will therefore be sufficient in what follows to restrict attention to the 'outer region' $r > a$; the stream function in the inner region $r < a$ may then immediately be inferred from (3.14).

Substitution of (3.10) in (3.6) now gives

$$\psi(r,\theta) = \frac{\omega a^2}{2\pi i}\int_{-1-i\infty}^{-1+i\infty}\left(\frac{a}{r}\right)^p \frac{1}{W(p)}\left[\frac{\cos(p+2)\alpha \sin p\theta}{p} - \frac{\cos p\alpha \sin(p+2)\theta}{p+2}\right]dp. \tag{3.15}$$

When $r > a$, this integral may be evaluated by closing the contour by a large semicircle in the right-hand half-plane $\mathrm{Re}\, p > -1$. The integrand has a removable singularity at $p = -1$, and poles at the other zeros of the function $W(p)$. We therefore have to locate these zeros, and calculate the corresponding residues. Further progress

† The condition of 'zero forcing at infinity' implicit in (3.1) may be relaxed somewhat without affecting the structure of the solution. In particular, if (3.1) is replaced by $u_\theta = \mp F(r)$ where $F(r) = o(r^{-\epsilon})$ at ∞, $o(r^{\epsilon})$ as $r \to 0$, then the same method of solution is applicable with very similar results.

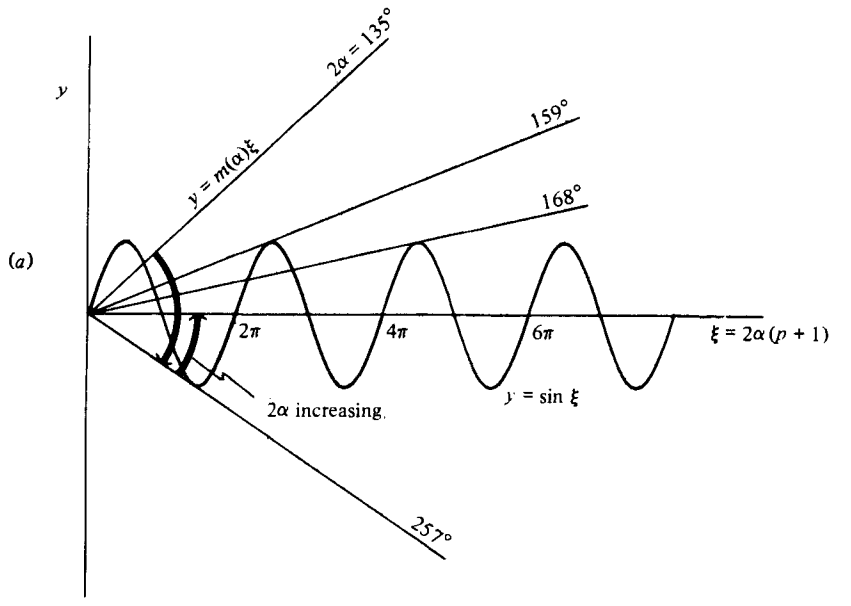

FIGURE 6(*a*). For legend see next page.

requires rather careful consideration of the function $W(p)$, which is analysed in the following section.

4. Zeros of the function $W(p)$, Re $p > -1$†

Consider first the real zeros of $W(p)$. Let $p+1 = \xi/2\alpha$; then

$$W = m(\alpha)\xi - \sin\xi, \quad m(\alpha) = \frac{\sin 2\alpha}{2\alpha}, \tag{4.1}$$

and the real zeros of $W(p)$ are given by the intersections of the straight line $L_\alpha: y = m(\alpha)\xi$ and the sine curve $S: y = \sin\xi$. These intersections are illustrated in figure 6(*a*) for various values of 2α. Note the following properties which may be easily inferred from the diagram.

(i) For $0 < 2\alpha < 2\alpha_1 \approx 159°$, there is only one real root, namely $\xi = 2\alpha$ (corresponding to $p = 0$). (This angle was incorrectly given as 156° in Moffatt 1964*a*; it is the angle below which corner eddies inevitably form in symmetric flow near the corner produced by some symmetric agitation at some distance from the corner.)

(ii) The angle $2\alpha_1$ is the first of a sequence of angles $\{2\alpha_n\}$ ($2\alpha_2 \approx 168°$, $2\alpha_3 \approx 172°$ and asymptotically $2\alpha_n \sim (4n+1)\pi^2/[(4n+1)\pi+2]$) for which L_α touches S. When $\alpha_n < \alpha < \alpha_{n+1}$, there are $2n+1$ real roots of $W(p) = 0$ with $p > -1$. When $\alpha = \alpha_n$, there are $2n$ such real roots, the largest being a double root. Obviously $2\alpha_n \to \pi$ as $n \to \infty$.

(iii) There is a second similar sequence of angles, $\{2\alpha_n'\}$ say, in the range

$$\pi < 2\alpha < 2\alpha_1' \approx 198°,$$

and a third similar sequence $\{2\alpha_n''\}$, in the range $2\alpha_1'' < 2\alpha < 2\pi$ (where $2\alpha_1'' \approx 328°$).

† The discussion of this section follows a standard pattern established by Hardy (1902).

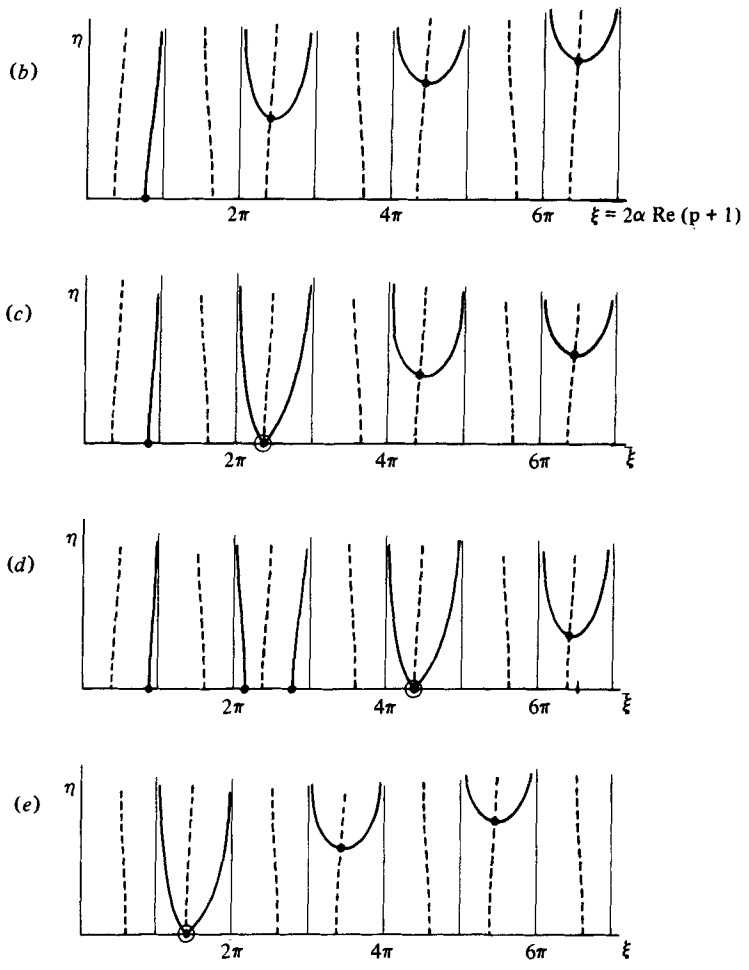

FIGURE 6. (*a*) The intersections of the straight line $y = m(\alpha)\,\xi$ and the sine curve $y = \sin\xi$ give the real zeros of $W(p)$. (*b*)–(*e*) Solid curves are the family defined by (4.4) and dashed curves are the family defined by (4.5). The intersections marked ● give the complex zeros of $W(p)$ with $\xi + i\eta = 2\alpha(p+1)$. Double zeros are indicated by ⊙. (*b*) $2\alpha = 135°$; (*c*) $2\alpha = 159°$; (*d*) $2\alpha = 168°$; (*e*) $2\alpha = 257°$.

(iv) When $2\alpha = 2\alpha_c \approx 257{\cdot}45°$ there is a double root of $W(p)$ at $p = 0$ ($\xi = 2\alpha_c$).

(v) For $2\alpha < 2\alpha_c$, the smallest root of $W(p)$ is $p = 0$; for $2\alpha > 2\alpha_c$, however, the smallest root p_1 satisfies

$$-\tfrac{1}{2} \leqslant p_1 < 0 \tag{4.2}$$

(with equality only at $2\alpha = 2\pi$).

Consider now the complex zeros of $W(p)$. Let

$$p + 1 = (\xi + i\eta)/2\alpha, \tag{4.3}$$

and suppose that $\eta \neq 0$. Since $W(p^*) = (W(p))^*$, the complex zeros occur in complex

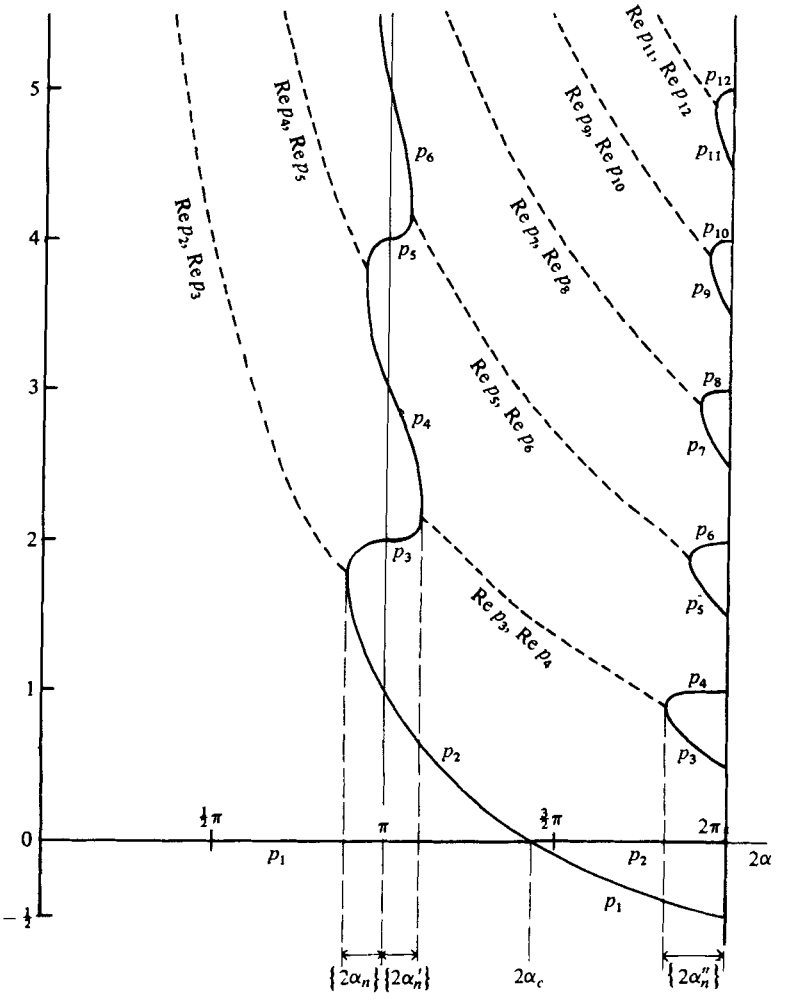

FIGURE 7. Sketch of variation of the first few zeros of $W(p)$ as functions of 2α. Where the curves are solid, p_n is real; where the curves are dashed, p_n is complex, and only the real part of p_n is represented.

conjugate pairs, and it will be sufficient to consider those in the first quadrant $\xi > 0$, $\eta > 0$. The real and imaginary parts of the equation $W(p) = 0$ may be written

$$\frac{\sin\xi}{\xi} = \frac{\sin 2\alpha}{2\alpha\cosh\eta}, \tag{4.4}$$

$$\frac{\sin 2\alpha}{2\alpha}\frac{\eta}{\sinh\eta} = \cos\xi. \tag{4.5}$$

For given α, equations (4.4) and (4.5) represent two families of curves in the (ξ, η) plane, and the intersections give the complex roots of $W(p)$. [The intersections of (4.4) with the real axis $\eta = 0$ give the real roots treated above.] These curves are sketched in figures 6(*b–e*) for the four particular choices of the angle 2α represented

by the lines L_α in figure 6(*a*). From such curves, we may infer the following properties of the zeros of $W(p)$.

(i) For $0 < 2\alpha < \pi$, in each strip S_{2n}, where S_m is defined by

$$S_m = \{\xi; m\pi < \xi < (m+1)\pi, \quad m = 1, 2, \ldots\},$$

there are either two real zeros of $W(p)$ (as discussed above) or two complex conjugate zeros. We shall denote the two zeros in the strip S_{2n} by p_{2n} and p_{2n+1}; if they are real then $p_{2n} \leqslant p_{2n+1}$ and if they are complex $p_{2n+1} = p_{2n}^*$ (and we may adopt the convention $\operatorname{Im} p_{2n} > 0$, $\operatorname{Im} p_{2n+1} < 0$).

(ii) For $\pi < 2\alpha < 2\pi$, in each strip S_{2n+1} ($n = 1, 2, 3, \ldots$) there are either two real zeros of $W(p)$ (p_{2n+1}, p_{2n+2}) or two complex conjugate zeros ($p_{2n+2} = p_{2n+1}^*$). In the strip S_1, there are always two real zeros ($p_1, p_2; p_1 \leqslant p_2$) which coalesce to form a double zero only for the critical angle $\alpha = \alpha_c$.

The behaviour of the roots $p_1, p_2, p_3, \ldots$ (or their real parts where they are complex) is indicated in figure 7, over the full range $0 < 2\alpha \leqslant 2\pi$. Note the position of the critical angle $2\alpha_c$ and the denumerable sets $\{2\alpha_n\}$, $\{2\alpha_n'\}$, $\{2\alpha_n''\}$ (with limit points π, π, 2π respectively) on this figure.

5. Asymptotic behaviour of the stream function (3.15)

We are now in a position to evaluate the integral (3.15). When $r > a$, the contour, closed by a large semicircle in the half-plane $\operatorname{Re} p > -1$, encloses all the poles p_n described in the previous section. Suppose first that α is such that all of these poles are simple (i.e. $\alpha \notin \{\alpha_n\} \cup \{\alpha_n'\} \cup \{\alpha_n''\} \cup \{\alpha_c\}$); then standard evaluation of (3.15) gives, for $r > a$,

$$\psi(r, \theta) = -\omega a^2 \sum_{n=1}^{\infty} \left(\frac{a}{r}\right)^{p_n} \frac{1}{W'(p_n)} \left[\frac{\cos(p_n+2)\alpha \sin p_n\theta}{p_n} - \frac{\cos p_n\alpha \sin(p_n+2)\theta}{p_n+2}\right], \tag{5.1}$$

and in this formula, since the poles are simple,

$$W'(p_n) = \sin 2\alpha - 2\alpha \cos 2(p_n+1)\alpha \neq 0. \tag{5.2}$$

Note that the complex terms of the series (5.1) occur in complex conjugate pairs. Note further that, from (5.1), for $r > a$,

$$\psi(r, \alpha) = \omega a^2 \sum_{n=1}^{\infty} \left(\frac{a}{r}\right)^{p_n} \frac{W(p_n)}{p_n(p_n+2)\, W'(p_n)} = \tfrac{1}{2}\omega a^2, \tag{5.3}$$

since $W(p_n) = 0$ and $\lim_{p \to 0} p^{-1} W(p) = W'(0)$. This provides a check for consistency with (3.2), since the total flux introduced through the boundaries is

$$\psi(r, \alpha) - \psi(r, -\alpha) = \omega a^2 = 2Q. \tag{5.4}$$

Equation (5.1) has the form

$$\psi(r, \theta) = \omega a^2 \sum_{n=1}^{\infty} \left(\frac{a}{r}\right)^{p_n} f_n(\theta), \quad r > a, \tag{5.5}$$

where $f_n(\theta)$ depends implicitly on α. The result (3.14) then gives the corresponding expansion

$$\psi(r, \theta) = \omega a^2 \sum_{n=1}^{\infty} \left(\frac{r}{a}\right)^{p_n+2} f_n(\theta), \quad r < a. \tag{5.6}$$

For $2\alpha < 2\alpha_c = 257{\cdot}45°$, $p_1 = 0$ and

$$f_1(\theta) = \frac{-\theta\cos 2\alpha + \frac{1}{2}\sin 2\theta}{\sin 2\alpha - 2\alpha\cos 2\alpha} = \tfrac{1}{2}f(\theta), \tag{5.7}$$

where $f(\theta)$ is as given by (1.9), and so (5.5) gives

$$\psi(r,\theta) \sim \tfrac{1}{2}\omega a^2 f(\theta) = Qf(\theta) \quad \text{for} \quad r \gg a, \tag{5.8}$$

i.e. the Jeffery–Hamel solution (1.10). Similarly (5.6) gives

$$\psi(r,\theta) \sim \tfrac{1}{2}\omega r^2 f(\theta), \quad r \ll a, \tag{5.9}$$

which is just the similarity solution given by (1.8).

For $2\alpha > 2\alpha_c$, however, as noted in § 4, the smallest root p_1 lies in the range

$$-\tfrac{1}{2} \leqslant p_1 < 0$$

(and $p_2 = 0$); hence

$$\psi(r,\theta) \sim \begin{cases} \omega a^2 (a/r)^{p_1} f_1(\theta), & r \gg a, \quad (5.10) \\ \omega r^2 (r/a)^{p_1} f_1(\theta), & r \ll a, \quad (5.11) \end{cases}$$

where now

$$f_1(\theta) = (W'(p_1))^{-1}\,[p_1^{-1}\cos(p_1+2)\alpha\sin p_1\theta - (p_1+2)^{-1}\cos p_1\alpha\sin(p_1+2)\theta], \tag{5.12}$$

and clearly we do *not* recover the similarity solutions in this situation. The forms (5.10) and (5.11) do however satisfy the basic requirements (3.7), since $p_1 \geqslant -\frac{1}{2}$.

In the Jeffery–Hamel limit ($a \to 0$, $\omega \to \infty$, Q constant), (5.10) gives, for any fixed r,

$$\psi(r,\theta) \sim 2Q(r/a)^{-p_1} f_1(\theta). \tag{5.13}$$

From this, we may construct a local Reynolds number

$$R \sim (Q/\nu)\,(r/a)^{-p_1}. \tag{5.14}$$

Since $p_1 < 0$ when $\alpha > \alpha_c$, it would therefore appear that $R \gg 1$ (in the limit $a \to 0$, r fixed) no matter what the magnitude of the *source* Reynolds number $2Q/\nu$ may be. Inertia forces are then of dominant importance for all r, and a low-Reynolds-number treatment of the Jeffery–Hamel problem for $\alpha > \alpha_c$ would appear to be quite untenable, no matter how small Q/ν may be.

As mentioned in the introduction, the breakdown of the Jeffery–Hamel solution at $\alpha = \alpha_c$ (when $R = 2Q/\nu \to 0$) was noted by Fraenkel (1962) who also described a similar behaviour at finite R (see also Fraenkel 1973). From Fraenkel's discussion, it emerges that there exists a domain $\mathscr{D}: \alpha < \alpha_c(R)$ in the α–R plane (with $\alpha_c(0) \approx 129°$), within which the Jeffery–Hamel stream function $\psi_J(\theta;\alpha,R)$ is a continuous function of α, and that $\psi_J \to \infty$ (for all θ) as $\alpha \uparrow \alpha_c(R)$. It may be conjectured from the discussion of the present paper that when $\alpha > \alpha_c(R)$, the Jeffery–Hamel solution is *irrelevant*, and that the flow for such angles must depend on the manner in which the source Q is distributed in the neighbourhood of the vertex, as well as on its net strength.

Returning now to the low-Reynolds-number limit, when $2\alpha = 2\alpha_c$, as noted earlier, W has a double zero at $p = 0$, i.e.

$$W'(0) = \sin 2\alpha - 2\alpha\cos 2\alpha = 0, \tag{5.15}$$

and so the integrand in (3.15) has a double pole at $p = 0$. The leading term of the

asymptotic expansion of ψ for $r \gg a$ comes from the residue at this double pole and, from (3.15), is given by

$$\psi(r,\theta) \sim \frac{-2\omega a^2}{W''(0)} \left\{ \frac{d}{dp} \left(\frac{a}{r}\right)^p \left[\frac{\cos(p+2)\alpha \sin p\theta}{p} - \frac{\cos p\alpha \sin(p+2)\theta}{p+2} \right] \right\}_{p=0}$$

$$= \frac{\omega a^2}{2\alpha_c^2 \sin 2\alpha_c} \left\{ \log\left(\frac{r}{a}\right) [\theta \cos 2\alpha_c - \tfrac{1}{2} \sin 2\theta] + [\tfrac{1}{2}\theta \cos 2\theta - \tfrac{1}{4} \sin 2\theta + \alpha_c \theta \sin 2\alpha_c] \right\} \tag{5.16}$$

[which again satisfies $\psi(r,\alpha) = \frac{1}{2}\omega a^2$, consistent with (3.2)]. Once again, as in the simpler problem treated in § 2, a term logarithmic in r appears when the angle 2α is critical. Here, the situation is closely analogous to that resolved in the elasticity context by Sternberg & Koiter (1958). For $r \ll a$, the correspondence (3.14) shows that $\psi \sim r^2 \log r$ as $r \to 0$ when $\alpha = \alpha_c$.

We now have the additional interesting complication that $W(p)$ has a double zero [and so the integrand in (3.15) has a double pole] whenever α takes one of the special values (of which there is a countable infinity) for which L_α is tangent to S (see the discussion of § 3). For example, when $2\alpha = 2\alpha_1 \approx 159°$, there is a double pole at $p_2 = p_3 \approx 1{\cdot}78$ and the second and third terms of the expansion (4.1) have to be replaced by

$$\frac{-2\omega a^2}{W''(p_2)} \left\{ \frac{d}{dp} \left(\frac{a}{r}\right)^p \left[\frac{\cos(p+2)\alpha \sin p\theta}{p} - \frac{\cos p\alpha \sin(p+2)\theta}{p+2} \right] \right\}_{p=p_2}, \tag{5.17}$$

giving a contribution proportional to $(a/r)^{p_2} \log(a/r)$ for $r > a$. This contribution is however dominated (when $r \gg a$) by the leading term of (5.1), which is (5.8) (with $2\alpha = 159°$). Similarly when α takes any of the special values α_n, α_n', α_n'' for which L_α touches S, evaluation of the residue at the corresponding double pole, p_m say, gives rise to a contribution to ψ proportional to $(a/r)^{p_m} \log(a/r)$; this is, however, always dominated by the terms of the series (5.1) with $n < m$.

	$2\alpha < 2\alpha_c \approx 257°$	$2\alpha = 2\alpha_c$	$2\alpha > 2\alpha_c$
Hinged plate limit $r/a \to 0$	r^2, then r^{p_3+2}	$r^2 \log(a/r)$, then r^2, then r^{p_3+2}	r^{p_1+2}, then r^2, then r^{p_3+2}
Jeffery–Hamel limit $r/a \to \infty$	r^0, then r^{-p_3}	$\log(r/a)$, then r^0, then r^{-p_3}	r^{-p_1}, then r^0, then r^{-p_3}

TABLE 2. Asymptotic dependence of $\psi(r,\theta)$ on r as $r/a \to 0$ and $r/a \to \infty$ for the problem defined by (3.3) and (3.4). The exponents p_1, p_2 and p_3 are the roots of $W(p) = 0$ ordered so that $-1 < p_1 < \mathrm{Re}\, p_2 < \mathrm{Re}\, p_3$ (figure 7). For $2\alpha > 2\alpha_c$, $-\frac{1}{2} \leqslant p_1 < 0$.

The conclusions of the above analysis are summarized in table 2, which shows the radial dependence of the leading terms in the asymptotic expansion of $\psi(r,\theta)$ for $r/a \to 0$ and $r/a \to \infty$ for the problem defined by (3.3) and (3.4). It should perhaps be emphasized that we have assumed throughout that the boundary conditions and resulting flow fields are symmetric about $\theta = 0$. If antisymmetric ingredients are included, then the conclusions of table 2 require modification (see concluding footnote of Sternberg & Koiter 1958). The antisymmetric ingredients can be important in

certain circumstances, and in particular in some of the situations envisaged by Jeffrey & Sherwood (1980).

The 'explosion' in the solution (1.8) at $2\alpha \approx 257°$ was originally drawn to our attention by Dr T. J. Pedley, whose provocative observation is gratefully acknowledged, as is a stimulating discussion of the phenomenon with Dr J. M. Rallison. The work is supported by S.R.C. Research Grant no. GR/A/5993.4.

REFERENCES

ALLEN, R. F. & BIGGIN, C. M. 1974 Longitudinal flow of a lenticular liquid filament down an inclined plane. *Phys. Fluids* **17**, 287–291.

BATCHELOR, G. K. 1956 On steady laminar flow with closed streamlines at large Reynolds number. *J. Fluid Mech.* **1**, 177–190.

BATCHELOR, G. K. 1967 *Introduction to Fluid Dynamics*. Cambridge University Press.

COLLINS, W. M. & DENNIS, S. C. R. 1976 Viscous eddies near a 90° and a 45° corner in flow through a curved tube of triangular cross-section. *J. Fluid Mech.* **76**, 417–432.

FRAENKEL, L. E. 1961 On corner eddies in plane inviscid shear flow. *J. Fluid Mech.* **11**, 400–406.

FRAENKEL, L. E. 1962 Laminar flow in symmetrical channels with slightly curved walls. I. On the Jeffery–Hamel solutions for flow between plane walls. *Proc. Roy. Soc.* A **267**, 119–138.

FRAENKEL, L. E. 1973 On a theory of laminar flow in channels of a certain class. *Proc. Camb. Phil. Soc.* **73**, 361–390.

HARDY, G. H. 1902 On the zeroes of the integral function $x - \sin x = \sum_{\infty}^{1} (-1)^{n-1} x^{2n+1}/(2n+1)!$ *Messenger of Math.* **31**, 161–165.

JEFFREY, D. J. & SHERWOOD, J. D. 1980 Streamline patterns and eddies in low-Reynolds-number flow. *J. Fluid Mech.* **96**, 315.

MOFFATT, H. K. 1964*a* Viscous and resistive eddies near a sharp corner. *J. Fluid Mech.* **18**, 1–18.

MOFFATT, H. K. 1964*b* Viscous eddies near a sharp corner. *Arch. Mech. Stosowanej* **16**, 365–372.

STERNBERG, E. & KOITER, W. T. 1958 The wedge under a concentrated couple: a paradox in the two-dimensional theory of elasticity. *J. Appl. Mech.* **25**, 575–581.

TRANTER, C. J. 1948 The use of the Mellin transform in finding the stress distribution in an infinite wedge. *Quart. J. Mech. Appl. Math.* **1**, 125–130.